Tryptophan Substitution of a Putative D4S6 Gating Hinge Alters Slow Inactivation in Cardiac Sodium Channels

Sho-Ya Wang,* Corinna Russell,† and Ging Kuo Wang†
*Department of Biology, State University of New York, Albany, New York 12222; and †Department of Anesthesia, Brigham and Women's Hospital and Harvard Medical School, Boston, Massachusetts 02115

ABSTRACT Voltage-gated Na^+ channels display rapid activation gating (opening) as well as fast and slow inactivation gating (closing) during depolarization. We substituted residue S1759 (serine), a putative D4S6 gating hinge of human cardiac hNav1.5 Na^+ channels with A (alanine), D (aspartate), K (lysine), L (leucine), P (proline), and W (tryptophan). Significant shifts in gating parameters for activation and steady-state fast inactivation were observed in A-, D-, K-, and W-substituted mutant Na^+ channels. No gating shifts occurred in the L-substituted mutant, whereas the P-substituted mutant did not yield sufficient Na^+ currents. Wild-type, A-, D-, and L-substituted mutant Na^+ channels showed little or no slow inactivation with a 10-s conditioning pulse ranging from −180 to 0 mV. Unexpectedly, W- and K-substituted mutant Na^+ channels displayed profound maximal slow inactivation around −100 mV (~85% and ~70%, respectively). However, slow inactivation was progressively reversed in magnitude from −70 to 0 mV. This regression was minimized in inactivation-deficient hNav1.5-S1759W/L409C/A410W Na^+ channels, indicating that the intracellular fast-inactivation gate caused such a reversal. Our data suggest that the hNav1.5-S1759 residue plays a critical role in slow inactivation. Possible mechanisms for S1759 involvement in slow inactivation and for antagonism between fast and slow inactivation are discussed.

INTRODUCTION

Mammalian voltage-gated Na^+ channels are membrane proteins consisting of one large α-subunit and one or two smaller β-subunits (Catterall, 2000). The Na^+ channel α-subunit contains four repeated domains (D1–D4) each with six transmembrane segments (S1–S6). Nine distinct Na^+ channel α-subunit isoforms have been identified in mammals. Gating characteristics of Na^+ channel isoforms appear to vary considerably, including activation gating that leads to rapid channel opening and fast and slow inactivation gating that lead to channel closing during brief and prolonged depolarization, respectively. Parts of the gating machinery, such as voltage sensors at four S4 segments responsible for Na^+ channel activation and the inherent fast-inactivation gate at the D3-D4 intracellular linker, have been delineated (Catterall, 2000).

In contrast, slow inactivation gating remains largely unknown (Vilin and Ruben, 2001). Slow inactivation of human cardiac hNav1.5 Na^+ channels is less complete than that in rat skeletal muscle rNav1.4 Na^+ channels (O'Reilly et al., 1999; Richmond et al., 1998). Defective slow inactivation in human cardiac Na^+ channels has been linked to Brugada syndrome (Veldkamp et al., 2000; Vilin et al., 2001). Slow inactivation of Na^+ channels was considerably accelerated after removal of fast inactivation, suggesting that this slow process occurs via a molecular entity different from that for fast inactivation (Rudy, 1978). Mutations at S5 segments (Cummins and Sigworth, 1996; Hayward et al., 1997), voltage sensors (Mitrovic et al., 2000; Struyk et al., 2000), P-loops (Hilber et al., 2002; Sandtner et al., 2004; Vilin et al., 1999), and S6 segments (Masanori and Cannon, 1999; O'Reilly et al., 2001; Wang and Wang, 1997) all appear to alter slow inactivation, but how these disparate regions affect slow inactivation gating is unclear.

Several groups suggest that a putative gating hinge (G, glycine in D1–D3, and S, serine in D4; Fig. 1, bracketed at position 12) is present at the middle of S6s of Na^+ channel isoforms (Sunami et al., 2004; Wang et al., 2003; Yarov-Yarovoy et al., 2002). The existence of such an S6 gating hinge in Na^+ channels is based on the structural homology with homotetrameric K^+ channels (G residue; Jiang et al., 2002). Both G and S residues belong to the α-helix breaking set of amino acids with low conformational preference to be in the middle of an α-helix (Chou and Fasman, 1978; Creighton, 1993). Using site-directed mutagenesis, we attempted to investigate whether the putative gating hinge, serine, at D4S6 in cardiac Na^+ channels (hNav1.5-S1759) plays a role in fast activation gating. Our results unexpectedly reveal that this S residue is also critical for slow inactivation gating.

MATERIALS AND METHODS

Site-directed mutagenesis

Human cardiac hNav1.5 cDNA clone was provided by Dr. Roland Kallen (University of Pennsylvania). We used QuikChange XL Site-Directed Mutagenesis Kit (Stratagene, La Jolla, CA) to substitute hNav1.5-S1759 in the pcDNA1 vector with A, D, K, L, P, and W residues as described (Wang et al., 2003). Two of these mutants, hNav1.5-S1759W and hNav1.5-S1759K, were also created in inactivation-deficient hNav1.5-L409C/A410W backbone channels. Mutations were confirmed by DNA sequencing at the mutated site.

Submitted January 26, 2005, and accepted for publication March 22, 2005.

Address reprint requests to Ging Kuo Wang, Dept. of Anesthesia, Brigham and Women's Hospital and Harvard Medical School, Boston, MA 02115. Tel.: 617-732-6886; Fax: 617-730-2801; E-mail: wang@zeus.bwh.harvard.edu.

0006-3495/05/06/3991/09 $2.00

doi: 10.1529/biophysj.105.059352

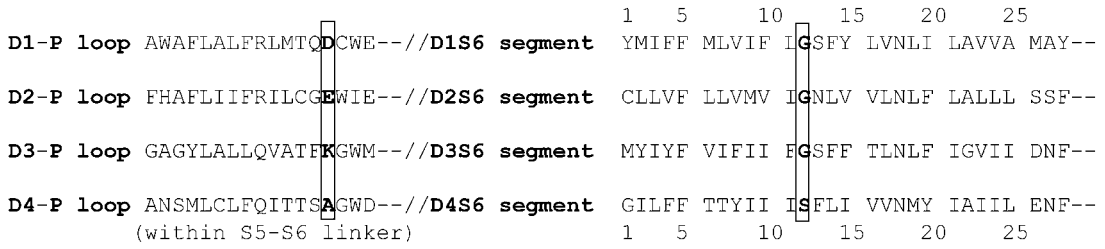

FIGURE 1 Amino acid sequences of P-loops and S6s of hNav1.5 α-subunit. The selectivity filter within the P-loops, i.e., the DEKA locus, is boxed. The gating hinge within S6s at position 12 is also boxed.

HEK293t cells and transient transfection

Human embryonic kidney cells (HEK293t) were grown to ~50% confluence in DMEM (Life Technologies, Rockville, MD) containing 10% fetal bovine serum (HyClone, Logan, UT), 1% penicillin, and streptomycin solution (Sigma, St. Louis, MO), 3 mM taurine, and 25 mM HEPES and then transfected by a calcium phosphate precipitation method. Transfection of hNav1.5-pcDNA1/Amp or mutant clones (5–10 μg) along with rat β1 (10–20 μg) and reporter CD8-pih3m (1 μg) was adequate for current recording. Cells were replated 15 hr after transfection in 35-mm dishes, maintained at 37°C in a 5% CO_2 incubator, and used after 1–4 days. Transfection-positive cells were identified with immunobeads (CD8 Dynabeads, Dynal, Lake Success, NY).

Electrophysiology and data acquisition

The whole-cell configuration of a patch-clamp technique (Hamill et al., 1981) was used to study Na^+ currents in HEK293 cells at room temperature (22 ± 2°C). Electrode resistance ranged from 0.5 to 1.0 MΩ. Command voltages were elicited with pCLAMP8 software and delivered by Axopatch 200B (Axon Instruments, Union City, CA) or by EPC-7 (HEKA Elektronik, Lambrecht, Germany). Cells were held at −140 mV and dialyzed for 10 to 15 min before current recording. The capacitance and leak currents were reduced by a patch-clamp device and by P/-4 subtraction. Liquid junction potential was not corrected. Access resistance was 1–2 MΩ under the whole-cell configuration; series resistance compensation of >85% typically resulted in voltage errors of ≤3 mV at +30 mV. Test pulses were generally applied at +30 mV for the outward Na^+ currents. Curve fitting was performed by Microcal Origin (Northampton, MA). An unpaired Student's *t*-test was used to evaluate estimated parameters (mean ± SE or fitted value ± SE of the fit); *P* values of <0.05 were considered statistically significant.

Solutions

Cells were perfused with an extracellular solution containing (in mM) 65 NaCl, 85 choline-Cl, 2 $CaCl_2$, and 10 HEPES (titrated with tetramethylammonium-OH to pH 7.4). The pipette (intracellular) solution consisted of (in mM) 100 NaF, 30 NaCl, 10 EGTA, and 10 HEPES (titrated with cesium-OH to pH 7.2). Recordings under this Na^+ gradient condition allowed us to avoid the complication of series resistance artifacts and to minimize inward Na^+ ion loading (Cota and Armstrong, 1989).

RESULTS

Activation and fast-inactivation gating in wild-type and hNav1.5-S1579A/D/K/L/W mutant channels

Families of superimposed Na^+ currents in wild-type and mutant hNav1.5 channels were generated at various voltages. Representative current traces of wild-type and hNav1.5-S1759W are shown in Fig. 2, *A* and *B*, respectively. The peak currents were measured, converted to conductance, normalized with respect to the value at +50 mV, and plotted against voltage (Fig. 2 *C*). The plot shows that Na^+ channels are activated around −70 mV and −60 mV for wild-type and hNav1.5-S1579W, respectively. The voltage that activated 50% of Na^+ channels ($E_{0.5}$) and the slope factor (k_E) measured −49.8 mV and 12.1 mV for wild-type and −39.4 mV and 11.3 mV for hNav1.5-S1579W, respectively. The activation gating parameters of other S1579 mutants are included in Table 1. The rightward shift by S1579W mutation was 10.4 mV ($P < 0.05$), but the slope factor was not significantly different from the wild-type ($P > 0.05$). Also rightward shifted in channel activation were S1579K mutant channels, whereas S1579A and D mutant channels were leftward shifted. The changes in activation were minimal for S1579L channels ($P > 0.05$). The S1579P mutant expressed poorly and was not characterized.

Steady-state fast inactivation (h_∞) was determined by a conventional two-pulse protocol. Superimposed representative current traces were generated at various conditioning pulses for wild-type and hNav1.5-S1759W shown in Fig. 3, *A* and *B*, respectively. The peak currents were measured, normalized with respect to the maximal value with the conditioning pulse at −160 mV, and plotted against the conditioning voltage (Fig. 3 *C*). The voltage that inactivated 50% of Na^+ channels ($h_{0.5}$) and the slope factor (k_h) measured −86.0 mV and 7.4 mV for wild-type and −94.9 and 7.6 mV for hNav1.5-S1579W, respectively. The gating parameters of steady-state inactivation in wild-type and various mutant channels are listed in Table 1. We found that, in contrast to activation, the steady-state inactivation was leftward shifted by 8.9 mV in the S1579W mutant. Similarly, the S1579K substitution elicited a leftward shift of 13.3 mV in steady-state inactivation, whereas the S1579A and D substitutions elicited a rightward shift of 9.1 mV and 4.4 mV, respectively. No significant shifts were observed in steady-state inactivation of hNav1.5-S1579L mutant channels ($P > 0.05$; Table 1) although its slope factor was reduced significantly ($P < 0.05$). None of the mutant channels displayed any noninactivating currents, suggesting that fast inactivation reaches its completion under our experimental conditions.

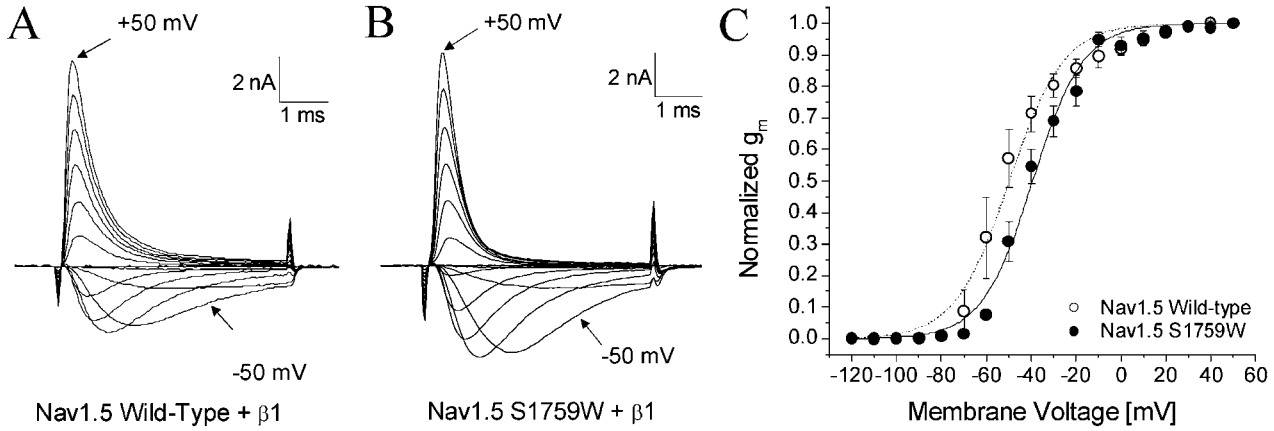

FIGURE 2 Activation gating of Nav1.5 wild-type and Nav1.5-S1759W. Currents were evoked by 5-ms test pulses from −120 mV to +50 mV in 10-mV increments for (*A*) Nav1.5 wild-type and (*B*) Nav1.5-S1759W. The inward current evoked by a −50 mV pulse and the outward current evoked by a +50 mV pulse are labeled. Normalized conductance (g_m) was plotted against the corresponding voltage. Gm was determined from the equation $g_m = I_{Na}/(E_m - E_{Na})$, where I_{Na} is the peak current, E_m is the amplitude of the voltage step, and E_{Na} is the estimated reversal potential of the Na^+ current. Plots were fitted with a Boltzmann function. The average midpoint voltage ($E_{0.5}$) and slope (k_E) of the function for Nav1.5 wild-type (○, $n = 5$) were −49.8 ± 1.2 mV and 12.1 ± 1.1 mV, respectively, and −39.4 ± 0.9 mV and 11.3 ± 0.8 mV for Nav1.5-S1759W (●, $n = 5$). All cells were cotransfected with the β1 subunit. Holding potential was set at −140 mV.

Slow inactivation in wild-type, hNav1.5/S1579A/D/K/L, and W mutant channels

We applied various conditioning pulses from −180 to 0 mV with a constant 10-s duration to determine whether significant changes in slow inactivation occur in these mutant channels (Fig. 5 *A*). An interpulse with a 100-ms duration at −140 mV holding potential was inserted to allow recovery from fast inactivation before a test pulse at +30 mV for 5 ms was applied. Under these conditions, slow inactivation was minimal in wild-type Na^+ channels as shown in Fig. 4 *A*. The peak currents were measured, normalized, and plotted against the conditioning voltages (Fig. 5, *open circles*); <10% of hNav1.5 Na^+ currents were slow inactivated even at the conditioning voltage of 0 mV. Like wild-type channels, hNav1.5-S1759A, D, and L mutant Na^+ channels displayed minimal slow inactivation (Fig. 5, *solid circles*, *solid triangles*, and *solid diamonds*, respectively).

In contrast, hNav1.5-S1759W mutant Na^+ channels displayed a very different pattern in slow inactivation. First, from −160 to −100 mV, slow inactivation increased progressively as the peak Na^+ currents at the test pulse continued to decrease to a level of ~15% of the maximal peak currents (Fig. 4 *B*). Second, from −80 to 0 mV, slow inactivation reversed its course and regressed progressively as the peak Na^+ current continued to increase to a level of ~80% of the maximal peak currents (Fig. 4 *C*). The V-shaped nature of slow inactivation in hNav1.5-S1759W mutant Na^+ channels is shown clearly in Fig. 5 (*open squares*). A V-shaped slow inactivation was also found in hNav1.5-S1759K mutant Na^+ channels but with some quantitative differences. The maximal level for slow inactivation in hNav1.5-S1759K mutant Na^+ channels was ~70% at −100 mV and the slow inactivation reversed to ~50% at 0 mV (Fig. 5, *downward triangles*).

Development of and recovery from slow inactivation of hNav1.5-S1759W and K mutants

To compare the entrance to and exit from the slow-inactivated state of wild-type and hNav1.5-S1759W and K mutant Na^+ channels, we measured their kinetics at −100 mV. Fig. 6 *A* shows the development of slow inactivation of wild-type,

TABLE 1 Activation and steady-state fast-inactivation (h_∞) gating of hNav1.5-S1759 mutant Na^+ channels

Channel type	Activation			Steady-state fast inactivation (h_∞)		
hNav1.5	$E_{0.5}$ (mV)	k_E (mV)	n	$h_{0.5}$ (mV)	k_h (mV)	n
Wild-type	−49.8 ± 1.2	12.1 ± 1.1	5	−86.0 ± 1.2	7.4 ± 0.2	5
S1759A	−59.8 ± 1.3* Δ −10.0	6.9 ± 1.1* Δ −5.2	5	−76.9 ± 1.3* Δ 9.1	5.6 ± 0.3* Δ −1.8	5
S1759D	−55.4 ± 0.9* Δ −5.6	10.5 ± 0.8 Δ −1.6	5	−81.6 ± 1.3* Δ 4.4	6.3 ± 0.3* Δ −1.1	5
S1759K	−42.6 ± 1.7* Δ 7.2	13.7 ± 1.5 Δ 1.6	5	−99.4 ± 1.4* Δ −13.4	10.7 ± 0.3* Δ 3.3	5
S1759L	−48.4 ± 1.1 Δ 1.4	11.3 ± 1.0 Δ −0.8	5	−84.7 ± 1.4 Δ 1.3	6.0 ± 0.3* Δ −1.4	5
S1759W	−39.4 ± 0.9* Δ 10.4	11.3 ± 0.8 Δ −0.8	5	−94.9 ± 1.2* Δ −8.9	7.6 ± 0.2 Δ 0.2	5

Parameters for activation ($E_{0.5}$ and k_E) and steady-state inactivation ($h_{0.5}$ and k_h) are described in Figs. 2 *C* and 3 *C*, respectively.
*$P < 0.05$, n is the number of experiments, and Δ represents the difference ($value_{mutant} - value_{wild\text{-}type}$).

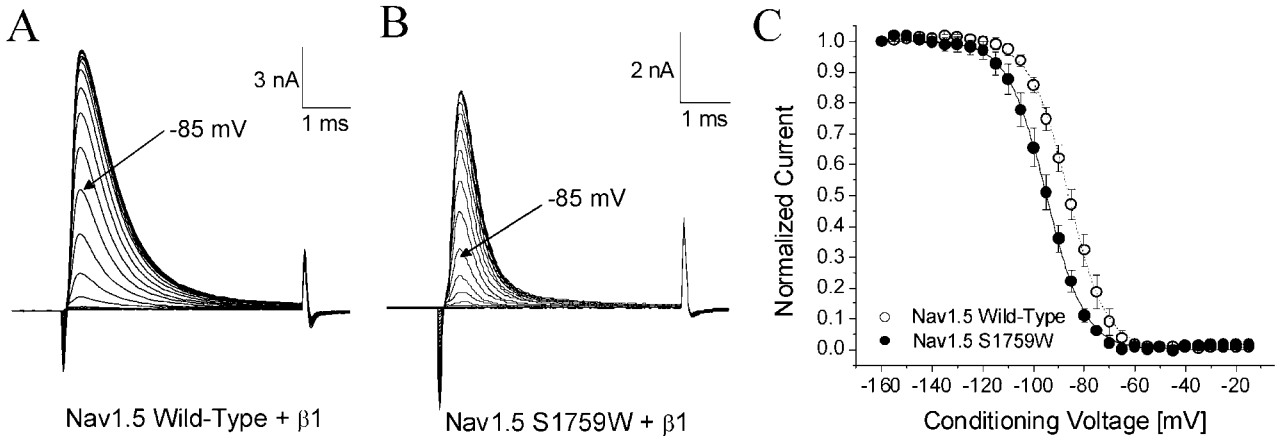

FIGURE 3 Steady-state inactivation of Nav1.5 wild-type and Nav1.5-S1759W. Currents were evoked by a 5-ms test pulse to +30 mV for (*A*) Nav1.5 wild-type and (*B*) Nav1.5-S1759W. Test pulses were preceded by 100-ms conditioning pulses, increased in 5-mV increments between −160 mV and −15 mV. (*C*) Normalized Na^+ current availability (h_∞) of Nav1.5 wild-type was plotted as a function of the conditioning voltage. Data were fitted with the Boltzmann function. The average midpoint ($h_{0.5}$) and slope factor (k_h) for the wild-type solution (○, $n = 5$) were −86.0 ± 1.2 mV and 7.4 ± 0.2 mV, respectively, and −94.9 ± 1.2 mV and 7.6 ± 0.2 mV for Nav1.5-S1759K (●, $n = 5$). Holding potential was set at −140 mV.

hNav1.5-S1759W, and K mutant channels in two different time frames. Slow inactivation of wild-type was minimal (~8%) at −100 mV with a time constant of ~15 s at this voltage. In comparison, slow inactivation of hNav1.5-S1759K reached 61.5% with fast and slow time constants of 0.12 s and 4.4 s, respectively, whereas slow inactivation of hNav1.5-S1759W mutant channels reached 81.2% with fast and slow time constants of 0.7 s and 10.8 s, respectively.

Fig. 6 *B* shows the time courses of recovery from slow inactivation at −180 mV for wild-type, hNav1.5-S1759K,

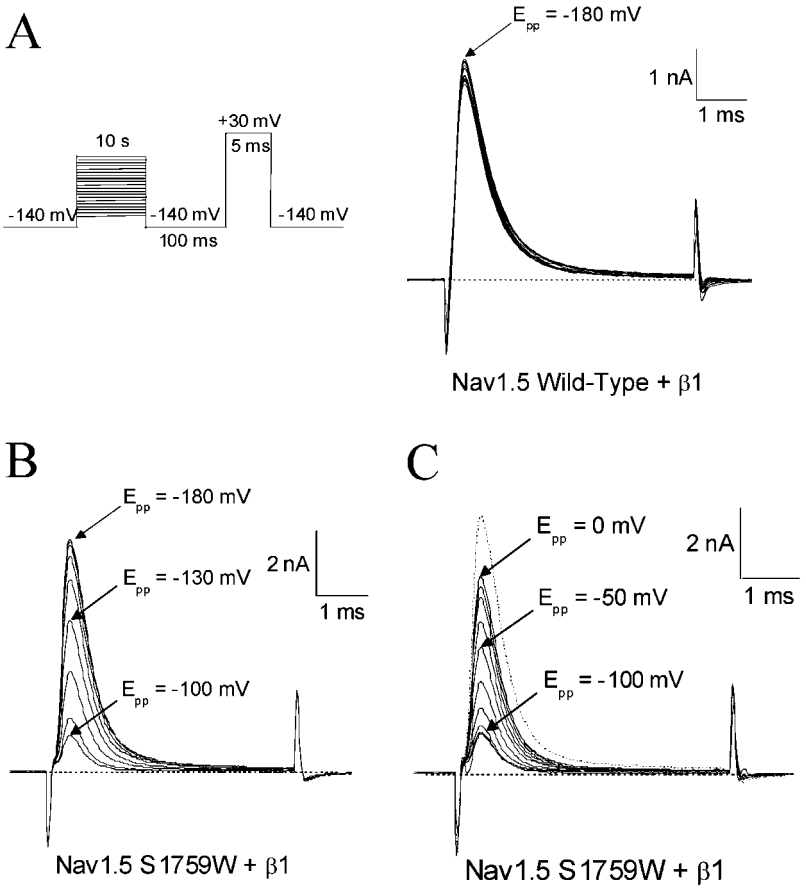

FIGURE 4 Slow inactivation of Nav1.5 wild-type and Nav1.5- S1759W. A 10-s conditioning prepulse ranging from −180 mV to 0 mV was first applied. After a 100-ms interval at −140 mV, Na^+ currents were evoked by a 5-ms test pulse at +30mV as shown in the inset. (*A*) Superimposed current traces for Nav1.5 wild-type show a <10% decrease in the peak amplitude. The current evoked after a −180 mV conditioning pulse is labeled. (*B*) Superimposed current traces for Nav1.5-S1759W for the first half of the experiment. The currents evoked after −180 mV, −130 mV, and −100mV conditioning pulses are labeled. After a −100 mV conditioning pulse, only 15% of the original current is evoked. (*C*) Superimposed current traces for Nav1.5 S1759W for the second half of the experiment. The −180 mV current trace (*B*) is shown as a dotted line. The currents evoked after −100 mV, −50 mV, and 0 mV conditioning pulses are labeled. After a 0 mV conditioning pulse, almost 80% of the original current has recovered.

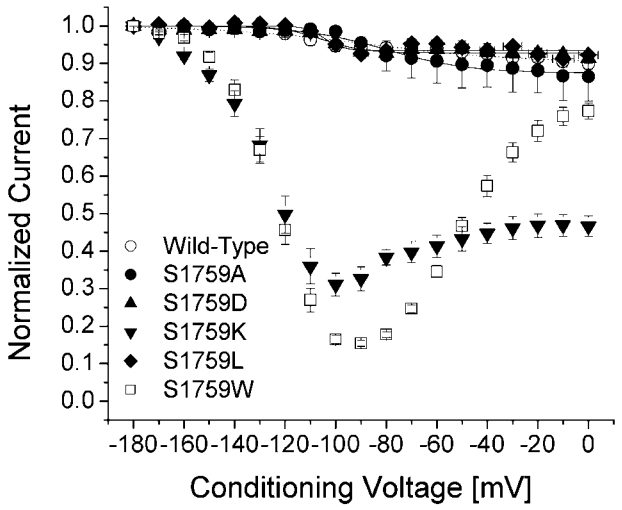

FIGURE 5 Slow inactivation of Nav1.5 wild-type and mutant channels. Data were obtained as in Fig. 4 and normalized to the peak amplitude after the −180 mV conditioning pulse. Normalized data were plotted against the conditioning prepulse voltages. Data were fitted with a Boltzmann function ($1/[1 + \exp((V_{0.5} - V)/K_E)]$). The average $V_{0.5}$ value and K_E (slope factor) and Y_0 values (in parentheses) for the fitted functions were −103.4 ± 5.1 mV and 12.8 ± 4.0 mV (0.92 ± 0.04), respectively, for Nav1.5 wild-type (○, $n = 6$); −80.1 ± 2.8 mV and 16.5 ± 2.8 mV (0.87 ± 0.05), respectively, for Nav1.5-S1759A (●, $n = 5$); −105.2 ± 2.6 mV and 8.1 ± 2.3 mV (0.93 ± 0.03), respectively, for Nav1.5-S1759D (▲, $n = 5$); and −104.6 ± 2.7 mV and 3.4 ± 1.9 mV (0.94 ± 0.03), respectively, for Nav1.5 S1759L (♦, $n = 5$). Plots for Nav1.5-S1759K (▼) and Nav1.5-1759W (◇) were not fitted well with a Boltzmann function.

and hNav1.5-S1759W mutant Na^+ channels. These recovery time courses were best fitted by a two-exponential function. Most wild-type channels recovered rapidly, whereas hNav1.5-S1759K mutant Na^+ channels recovered significantly more slowly and hNav1.5-S1759W was the slowest. The kinetic results from the development of and recovery from slow inactivation indicate that there are multiple slow-inactivated states present in hNav1.5-S1759K and in hNav1.5-S1759W mutant channels. Substitutions of S with K or W appear to stabilize these slow-inactivated states drastically even at −100 mV where the wild-type hNav1.5 Na^+ channels show minimal slow inactivation.

Slow inactivation in hNav1.5-L409C/A410W and hNav1.5-S1759W/L409C/A410W inactivation-deficient mutant channels

A coarse correlation ($r = 0.61$) between slow inactivation and noninactivating Na^+ currents in various rNav1.4 S6 mutant channels was reported previously (Wang et al., 2003). To study the role of fast inactivation in the phenotype of slow inactivation of hNav1.5 wild-type and hNav1.5-S1759W, we created inactivation-deficient channels (hNav1.5-L409C/A410W, hNav1.5-S1759W/L409C/A410W, and hNav1.5-S1759K/L409C/A410W). The expression of W mutant channels with CW backbone in HEK293t cells is modest, generally ≤5 nA, whereas the expression of hNav1.5-L409C/A410W mutant channels is robust. The inactivation-deficient phenotype of hNav1.5-L409C/A410W channels is similar to that of rNav1.4-L437C/A438W counterparts (Wang et al., 2003). Mutant channels, hNav1.5-S1759K/L409C/A410W, failed to express sufficient Na^+ currents. Fig. 7 shows that normalized Na^+ currents at the test pulse begin to decline progressively at voltage >−60 mV, or around the activation threshold of mutant Na^+ channels, during prolonged depolarization (*open circles*) in hNav1.5-L409C/A410W inactivation-deficient mutant channels. Since such a phenotype does not occur in wild-type channels (*dotted line*), this result suggests that opening of mutant Na^+ channels enhances slow inactivation. In other words, the fast-inactivation gate antagonizes slow inactivation of cardiac Na^+ channels effectively, consistent with a well-known phenomenon described in squid axon treated with pronase (Rudy, 1978). These results therefore show that slow inactivation of wild-type cardiac hNav1.5 Na^+ channels does not occur readily in the resting and fast-inactivated states.

In comparison, the hNav1.5-S1759W/L409C/A410W inactivation-deficient mutant channels display a distinct enhanced slow inactivation as shown in Fig. 7 (*solid circles*). Again, S1759W mutation enhances slow inactivation drastically in hNav1.5-L409C/A410W mutant channels (*open* versus *solid circles*, Fig. 7). Of normalized currents, ~50% were slow inactivated at −140 mV, or a leftward shift of 85 mV, compared with hNav1.5-L409C/A410W mutant channels. One difference between hNav1.5-S1759W and hNav1.5-S1759W/L409C/A410W channels is also evident. The second rising phase shown in Fig. 4 for hNav1.5-S1759W is nearly reversed (*dashed line*), as if L409A/A410W substitutions impose an enhanced slow inactivation on the hNav1.5-S1759W channels from −60 to 0 mV. The reason for this unusual phenotype will be addressed in the Discussion.

DISCUSSION

By site-directed mutagenesis, we investigated the role of the putative D4S6 gating hinge (hNav1.5-S1759) in gating properties of cardiac Na^+ channels. Substitutions of S→W/K caused a significant rightward shift in activation and a significant leftward shift in steady-state fast inactivation. Unexpectedly, slow inactivation was enhanced in a V-shaped voltage-dependent manner in these mutants. In contrast, S→A/D substitutions did not enhance slow-inactivation gating significantly under identical conditions but did cause opposite shifts in activation and in steady-state fast inactivation compared with S→K/W substitutions. No gating shifts were found in S→L, whereas poor expression occurred in S→P.

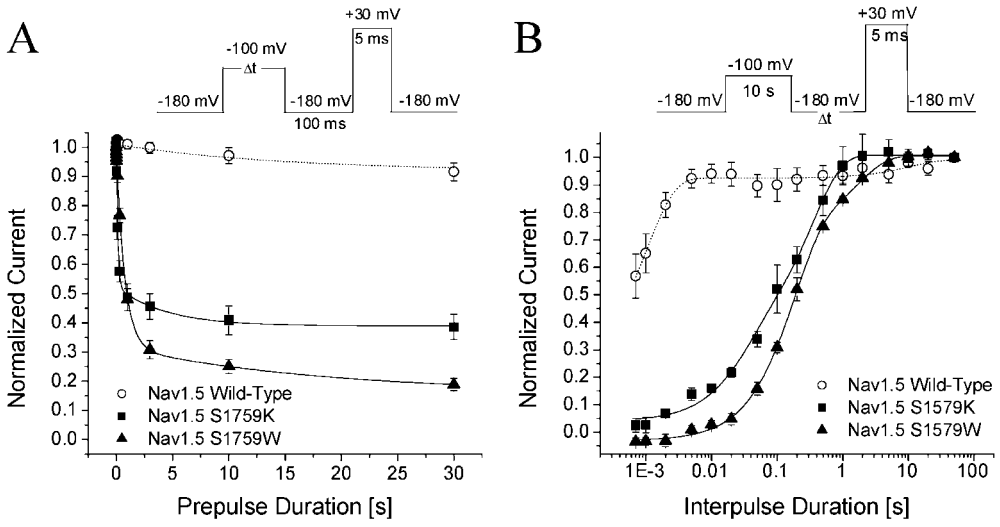

FIGURE 6 Development of and recovery from slow inactivation. (*A*) For the development of slow inactivation, a pulse protocol shown in the inset was applied. The peak currents at the test pulse were measured and normalized to the initial peak amplitude ($t = 0$) and plotted against the prepulse duration. The data were fitted by a single-exponential or, when appropriate, a double-exponential function. Time constants (and final Y_0 values in %) for Nav1.5 wild-type (○, $n = 5$), Nav1.5-S1759K (■, $n = 5$), and Nav1.5-S1759W (▲, $n = 5$) were 15.0 ± 13.4 s (91.7 ± 3.7%), (t_1) 0.12 ± 0.01 s, (t_2) 4.4 ± 2.1 s (38.5 ± 1.4%), and (t_1) 0.70 ± 0.04 s, (t_2) 10.8 ± 2.8 s (18.8 ± 0%), respectively. Cells were held at −180 mV. (*B*) The recovery from slow inactivation was measured by the pulse protocol shown in the inset. The peak currents at the test pulse were measured, normalized, and plotted against the interpulse duration. The recovery time courses were fitted by the sum of two exponentials. The fast and slow time constants were 0.0010 ± 0.0002 s and 10.5 ± 7.8 s (wild-type, ○, $n = 5$), 0.40 ± 0.05 s and 0.030 ± 0.009 s (S1759K, ■, $n = 5$), and 1.7 ± 0.3 s and 0.20 ± 0.01 s (S1759W, ▲, $n = 5$). Cells were held at −180 mV. We noticed that during a 10-s conditioning pulse nonlinear leak currents might arise in some cells. Such nonlinear leak could not be corrected by the P/-4 protocol.

Shifts in activation and steady-state fast inactivation by mutations at the putative D4S6 gating hinge

Recent studies have shown that alanine substitutions along S6 segments cause periodic shifts in activation and in steady-state fast inactivation (Yarov-Yarovoy et al., 2001, 2002). Such findings support the notion that S6s are critical for both activation and fast-inactivation gating. Because activation and fast-inactivation processes involve many different structural parts of the Na^+ channel and because these two fast gating processes are coupled (Catterall, 2000), it is difficult to discern whether concurrent effects on gating properties (Table 1) are due to the specific S1759 mutation directly, indirectly, or both. McPhee et al. (1995) reported that a substitution of the rNav1.2-S1763A residue (homologous to hNav1.5-S1759A) caused little change in activation and ~6 mV rightward shift in the steady-state fast inactivation in a frog oocyte expression system. These mutational effects were considerably less than those found in hNav1.5-S1759A Na^+ channels (Table 1). The reason for these deviations is unclear but could be due to different isoforms, expression systems, ionic compositions, and/or coexpression of $\beta 1$ subunit in HEK293t cells. Interestingly, we found no correlation between α-helical propensities of substituted residues (Chou and Fasman, 1974) and activation gating in mutant Na^+ channels (Table 1): A (1.45; leftward shift in activation), L (1.34; no shift), W (1.14; rightward), K (1.07; rightward), and D (0.98; leftward). In fact, serine found in wild-type channels has the lowest α-helical propensity (0.79) among these substituted residues. The reason for the lack of correlation between activation gating (Fig. 8) and α-helical propensities of substituted residues is unclear. One possible explanation is that the gating hinge and/or nearby S6 residues also interact with adjacent structures, such as the P-loops during fast activation gating. Alternatively, activation may require no significant movement of the D4S6 gating hinge since it may be less mobile (Yarov-Yarovoy et al., 2002). If true, mutational effects of residue S1759 on activation could be rather nonspecific.

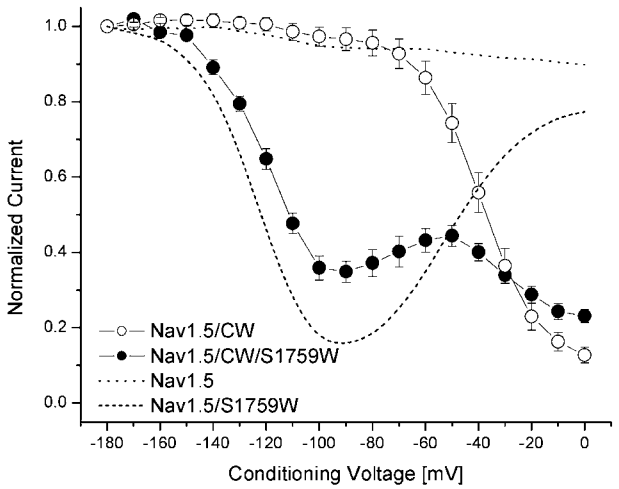

FIGURE 7 Voltage dependence of slow inactivation in inactivation-deficient hNav1.5-CW (○) and hNav1.5-CW/S1759W (●) mutant Na^+ channels. Inactivation-deficient Na^+ currents were recorded with an identical pulse protocol as shown in Fig. 4 *A*, and data were analyzed as described in Fig. 5; $n = 6$ and 5 for open and solid circles, respectively. For comparison, wild-type hNav1.5 (*dotted line*) and hNav1.5-S1759W mutant Na^+ channels are shown.

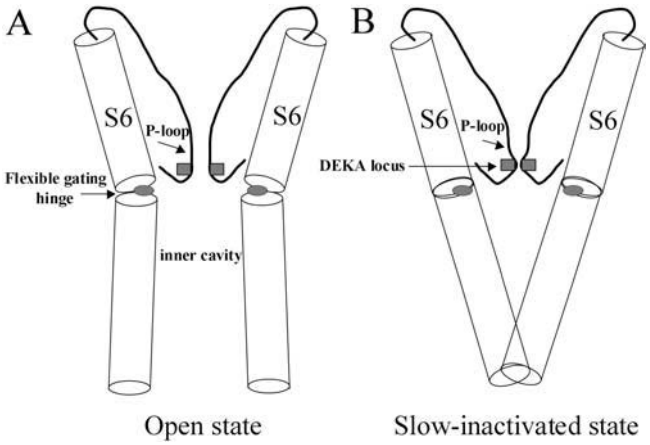

FIGURE 8 Cartoon of P-loop and S6 configurations within the open state (*A*) and slow-inactivated state (*B*) of Na^+ channels. Regions with shaded squares and ovals represent the selectivity filter (i.e., the DEKA locus) and the gating hinge (G or S residue), respectively. The gating hinge and/or nearby S6 residues may interact with amino acids at the adjacent P-loop. The DEKA locus and the S6 C-terminus are possible constriction sites for slow inactivation. The front and back P-loops and S6s are removed for clarity. Notice that the inner cavity is smaller in the slow-inactivated state when the S6s are in straight configurations. Sequences of P-loops and S6s are listed in Fig. 1. The intracellular fast-inactivation gate (not shown) occludes the permeation pathway, possibly via the inner cavity.

Altered slow inactivation by W/K substitutions at the D4S6 gating hinge

Cardiac hNav1.5 Na^+ channels are less prone to slow inactivation than skeletal muscle rNav1.4 isoforms (O'Reilly et al., 1999; Richmond et al., 1998). Although S→A/D substitutions did not enhance slow inactivation using our 10-s pulse protocol (Fig. 5), subtle differences in slow inactivation could be present among wild-type, S1759A, and S1759D channels when longer pulses (e.g., 300 s) were used in the assay. We did not expect that S→W/K substitutions at the D4S6 gating hinge would alter slow inactivation so drastically (Fig. 4), nor did we foresee the unique V-shaped voltage dependence of enhanced slow inactivation in these two mutants (Fig. 5). It is interesting that both hNav1.5-S1759W and S1759K mutant Na^+ channels display a leftward shift of steady-state inactivation with an $h_{0.5}$ value ~ -100 mV (shifts of 8.9 and 13.4 mV, respectively; Table 1), where their maximal slow inactivation also occurred. Such a result implies that opening of the Na^+ channels alone is unlikely to be a prerequisite for enhanced slow inactivation, since the threshold for activation gating is ~ -60 mV (Fig. 2 *C*).

Kinetic analyses of the development of and recovery from enhanced slow inactivation in these mutants indicate that there are multiple slow-inactivated states present as found in wild-type cardiac Na^+ channels (O'Reilly et al., 1999). Our data also show that substitutions of the serine residue at the D4S6 gating hinge with tryptophan and lysine cause significant changes in slow inactivation but not by other amino acid substitutions (Fig. 5). The serine residue at the hNav1.5-S1759 position is conserved in all nine mammalian Na^+ channel isoforms. Whether other Na^+ channel isoforms display similar enhanced slow inactivation by W and K substitutions at this gating hinge position remains to be seen.

Mechanism underlying the reversal of slow inactivation at 0 mV in hNav1.5-S1759W

The voltage dependence of slow inactivation in hNav1.5-S1759W is strongly V-shaped, unlike that in the wild-type (O'Reilly et al., 1999; Vilin and Ruben, 2001). The reversal of slow inactivation between −60 and 0 mV (Fig. 5) seems to overlap considerably with the voltage dependence of activation gating (Fig. 2). What could be the mechanism underlying the reversal of slow inactivation in hNav1.5-S1759W mutant?

The intrinsic fast-inactivation gate is capable of antagonizing slow inactivation of Na^+ channels (Hilber et al., 2002; Rudy, 1978). However, there are two types of fast inactivation: closed-channel fast inactivation, which is strongly voltage-dependent, and open-channel fast inactivation, which is voltage-independent (Aldrich and Stevens, 1983). It is likely that slow inactivation occurs maximally around −100 mV in hNav1.5-S1759W/K mutant Na^+ channels since the open-channel fast inactivation does not yet take place at this voltage range. At 0 mV, the open-channel fast inactivation occurs rapidly when the intrinsic fast-inactivation gate occludes the permeation pathway, possibly via the inner cavity (Zhou et al., 2001). If such an occlusion process within the inner cavity is hampered, slow inactivation can proceed readily. Our experiments in inactivation-deficient Na^+ channels (Fig. 7, *open circles*) support this interpretation. Inactivation-deficient Na^+ channels display enhanced slow inactivation progressively from −60 to 0 mV as if activation (opening) of Na^+ channels enhances slow inactivation. An additional mutation, hNav1.5-CW/S1759W, also renders the reversal of slow inactivation at 0 mV in hNav1.5-S1759W unattainable (Fig. 7, *solid circles*). Evidently, inactivation-deficient Na^+ channels enter their slow-inactivated state efficiently via their open state, a phenomenon predicted by Rudy (1978). Nonetheless, as discussed before channel opening alone is not necessarily required for slow inactivation since for hNav1.5-S1759W mutant Na^+ channels slow inactivation occurs maximally at −100 mV.

It can also be argued that the enhanced inactivation in hNav1.5-S1759W occurs as a mutational artifact. Accordingly, the gating hinge S1759W at D4S6 moves slowly to a new nonconducting state at −100 mV, which is unrelated to the traditional slow-inactivation process. This unique slow movement of S1759W during a prolonged pulse is apparently antagonized by the fast-inactivation gate (Fig. 7). Unfortunately, our results cannot distinguish these two alternatives. Further studies using pharmacological approaches (e.g., Hilber et al., 2002; Sandtner et al., 2004) may help address this question.

Possible mechanisms for the altered slow inactivation by S→K/W mutations at the putative gating hinge

Slow inactivation likely takes place via a constriction of the ion channel permeation pathway (Yellen, 1998). Besides the occlusion by the intrinsic fast-inactivation gate, there are a number of possible constriction sites to close the Na^+ channel (Fig. 8): 1), the external mouth of the permeation pathway, 2); the selectivity filter (DEKA locus), 3); the internal mouth, and 4); a combination of the above.

Struyk and Cannon (2002) studied the possibility of the constriction at the external Na^+ pore during slow inactivation and found that substituted cysteine residues adjacent to the external surface of the DEKA region remain accessible to charged cysteine-modifying reagents during slow inactivation. These authors suggested that the external pore region is not constricted in the slow-inactivated state. The possibility of the constriction at the DEKA locus during slow inactivation, however, remains viable (Fig. 8; Sandtner et al., 2004; Struyk and Cannon, 2002). The structural model of closed Na^+ channels proposed by Lipkind and Fozzard (2000) indicates that the S residue at D4S6 (rNav1.4-S1578) is close (~9 Å) to the K residue at the DEKA locus. It is therefore feasible that during prolonged depolarization the gating hinge region at D4S6 influences the DEKA locus or its adjacent residues and forces this site to become constricted. In fact, Hilber et al. (2002) recently described an enhanced ultra slow inactivation of rNav1.4-A1529D mutant skeletal muscle Na^+ channels expressed in frog oocytes. This A→D mutation was at the DEKA locus (alanine at D4). Interestingly, the voltage dependence of this enhanced ultra slow inactivation was similarly U-shaped in rNav1.4-A1529D mutant channels, although with a minimum near −60 mV. These authors suggested that ultra slow inactivation could occur via partially activated closed state and that the P-loop in D4 could undergo a slow conformational change during depolarization.

Alternatively, reclosure of S6 C-termini can also stop current flow during prolonged depolarization. This mechanism is suggested by Shin et al. (2004), who reported the S6 reclosure of the activation gate in HCN K^+ channels. Such a reclosure during depolarization, however, requires uncoupling between the voltage sensor and the S6 activation gate. Consistent with this mechanism, Jiang et al. (2003) reported that the volume of the inner cavity became smaller in the slow-inactivated state of Kv1.4 K^+ channels, as if S6 C-termini become reconstricted (Fig. 8 *B*). Furthermore, the activation gating hinge is found energetically stable in a straight configuration (Yifrach and MacKinnon, 2002). The substituted tryptophan residue (S1759W), which has an α-helical propensity of 1.14, is more stable in the straight S6 configuration than the serine residue (0.79). Nonetheless, the α-helical propensity alone cannot be the sole factor for the enhanced slow inactivation. Leucine (1.34) and alanine (1.45) have greater α-helical propensities than tryptophan but fail to enhance slow inactivation. This lack of correlation once more suggests that the gating hinge is likely to interact with adjacent amino acids during slow inactivation. Additional experiments are needed to address the precise mechanism for enhanced slow inactivation in hNav1.5-S1759W/K mutants and to reveal where the constriction site for slow inactivation is. Regardless of the answers, our data clearly show that the D4S6 gating hinge plays a pivotal role in slow inactivation gating.

We are grateful to Dr. Roland Kallen for providing us the hNav1.5 clone (hH1).

This work was supported by National Institutes of Health (GM 48090 and HL66076).

REFERENCES

Aldrich, R. W., and C. F. Stevens. 1983. Inactivation of open and closed sodium channels determined separately. *Cold Spring Harb. Symp. Quant. Biol.* 47:147–153.

Catterall, W. A. 2000. From ionic currents to molecular mechanisms: the structure and function of voltage-gated sodium channels. *Neuron.* 26: 13–25.

Chou, P. Y., and G. D. Fasman. 1974. Prediction of protein conformation. *Biochemistry.* 13:222–244.

Chou, P. Y., and G. D. Fasman. 1978. Empirical predictions of protein conformation. *Annu Rev Biochem.* 47:251–276.

Cota, G., and C. M. Armstrong. 1989. Sodium channel gating in clonal pituitary cells: the inactivation step is not voltage dependent. *J. Gen. Physiol.* 94:213–232.

Creighton, E. E. 1993. Protein, structures and molecular properties, 2nd ed. W. H. Freeman, New York.

Cummins, T. R., and F. J. Sigworth. 1996. Impaired slow inactivation in mutant Na^+ channels. *Biophys. J.* 71:227–236.

Hamill, O. P., E. Marty, M. E. Neher, B. Sakmann, and F. J. Sigworth. 1981. Improved patch-clamp techniques for high-resolution current recording from cells and cell-free membrane patches. *Pflugers Arch.* 391: 85–100.

Hayward, L. J., R. H. Brown, and S. C. Cannon. 1997. Slow inactivation differs among mutant Na channels associated with myotonia and periodic paralysis. *Biophys. J.* 72:1204–1219.

Hilber, K., W. Sandtner, O. Kudlacek, B. Schreiner, I. Glasser, W. Schutz, H. A. Fozzard, S. C. Dudley, and H. Todt. 2002. Interaction between fast and ultra-slow inactivation in the voltage-gated sodium channel. *J. Biol. Chem.* 277:37105–37115.

Jiang, X., G. C. Bett, X. Li, V. E. Bondarenko, and R. L. Rasmusson. 2003. C-type inactivation involves a significant decrease in the intracellular aqueous pore volume of Kv1.4 K^+ channels expressed in *Xenopus* oocytes. *J. Physiol.* 549:683–695.

Jiang, Y., A. Lee, J. Chen, M. Cadene, B. T. Chait, and R. MacKinnon. 2002. The open pore conformation of potassium channels. *Nature.* 417: 523–526.

Lipkind, G. M., and H. A. Fozzard. 2000. KcsA crystal structure as framework for a molecular model of the Na^+ channel pore. *Biochemistry.* 39:8161–8170.

Masanori, P., and S. C. Cannon. 1999. Enhanced slow inactivation by V445M: a sodium channel mutation associated with myotonia. *Biophys. J.* 76:861–868.

McPhee, J. C., D. S. Ragsdale, T. Scheuer, and W. A. Catterall. 1995. A critical role for transmembrane segment IVS6 of the sodium channel alpha subunit in fast inactivation. *J. Biol. Chem.* 270:12025–12034.

Mitrovic, N., A. L. George, and R. Horn. 2000. Role of domain 4 in sodium channel slow inactivation. *J. Gen. Physiol.* 115:707–717.

O'Reilly, J. P., S. Y. Wang, R. G. Kallen, and G. K. Wang. 1999. Comparison of slow inactivation in human heart and rat skeletal muscle Na^+ channel chimaeras. *J. Physiol.* 515:61–73.

O'Reilly, J. P., S. Y. Wang, and G. K. Wang. 2001. Residue-specific effects on slow inactivation at V787 in D2–S6 of Na(v)1.4 sodium channels. *Biophys. J.* 81:2100–2111.

Richmond, J. E., D. E. Featherstone, H. A. Hartmann, and P. C. Ruben. 1998. Slow inactivation in human cardiac sodium channels. *Biophys. J.* 74:2945–2952.

Rudy, B. 1978. Slow inactivation of the sodium conductance in squid giant axons. Pronase resistance. *J. Physiol.* 283:1–21.

Sandtner, W., J. Szendroedi, T. Zarrabi, E. Zebedin, K. Hilber, I. W. Glaaser, H. A. Fozzard, S. C. Dudley, and H. Todt. 2004. Lidocaine: a foot in the door of the inner vestibule prevents ultra-slow inactivation of a voltage-gated sodium channel. *Mol. Pharmacol.* 66:648–657.

Shin, K. S., C. Maertens, C. Proenza, B. S. Rothberg, and G. Yellen. 2004. Inactivation in HCN channels results from reclosure of the activation gate: desensitization to voltage. *Neuron.* 41:737–744.

Struyk, A. F., and S. C. Cannon. 2002. Slow inactivation does not block the aqueous accessibility to the outer pore of voltage-gated Na channels. *J. Gen. Physiol.* 120:509–516.

Struyk, A. F., K. A. Scoggan, D. E. Bulman, and S. C. Cannon. 2000. The human skeletal muscle Na channel mutation R669H associated with hypokalemic periodic paralysis enhances slow inactivation. *J. Neurosci.* 20:8610–8617.

Sunami, A., A. Tracey, I. W. Glaaser, G. M. Lipkind, D. A. Hanck, and H. A. Fozzard. 2004. Accessibility of mid-segment domain IV S6 residues of the voltage-gated Na^+ channel to methanethiosulfonate reagents. *J. Physiol.* 561:403–413.

Veldkamp, M. W., P. C. Viswanathan, C. R. Bezzina, A. Baartscheer, A. A. Wilde, and J. R. Balser. 2000. Two distinct congenital arrhythmias evoked by a multidysfunctional Na^+ channel. *Circ. Res.* 86:E91–E97.

Vilin, Y. Y., E. Fujimoto, and P. C. Ruben. 2001. A novel mechanism associated with idiopathic ventricular fibrillation (IVF) mutations R1232W and T1620M in human cardiac sodium channels. *Pflugers Arch.* 442:204–211.

Vilin, Y. Y., N. Makita, A. L. George, and P. C. Ruben. 1999. Structural determinants of slow inactivation in human cardiac and skeletal muscle sodium channels. *Biophys. J.* 77:1384–1393.

Vilin, Y. Y., and P. C. Ruben. 2001. Slow inactivation in voltage-gated sodium channels. *Cell Biochem. Biophys.* 35:171–190.

Wang, S.-Y., K. Bonner, C. Russell, and G. K. Wang. 2003. Tryptophan scanning of D1S6 and D4S6 C-termini in voltage-gated sodium channels. *Biophys. J.* 85:911–920.

Wang, S.-Y., and G. K. Wang. 1997. A mutation in segment I-S6 alters slow inactivation of sodium channels. *Biophys. J.* 72:1633–1640.

Yarov-Yarovoy, V., J. Brown, E. Sharp, J. J. Clare, T. Scheuer, and W. A. Catterall. 2001. Molecular determinants of voltage-dependent gating and binding of pore-blocking drugs in transmembrane segment IIIS6 of the Na^+ channel α subunit. *J. Biol. Chem.* 276:20–27.

Yarov-Yarovoy, V., J. C. McPhee, D. Idsvoog, C. Pate, T. Scheuer, and W. A. Catterall. 2002. Role of amino acid residues in transmembrane segments IS6 and IIS6 of the Na^+ channel α subunit in voltage-dependent gating and drug block. *J. Biol. Chem.* 277:35393–35401.

Yellen, G. 1998. The moving parts of voltage-gated ion channels. *Q. Rev. Biophys.* 31:239–295.

Yifrach, O., and R. MacKinnon. 2002. Energetics of pore opening in a voltage-gated K^+ channel. *Cell.* 111:231–239.

Zhou, M., J. H. Morals-Cabral, S. Mann, and R. MacKinnon. 2001. Potassium channel receptor site for the inactivation gate and quaternary amine inhibitors. *Nature.* 411:657–661.